Desalination and Water Treatment
www.deswater.com

doi: 10.5004/dwt.2021.26978

218 (2021) 352–362
April

Removal of Cd(II) ions in solution by activated carbon from palm oil shells modified with magnetite

Buhani[a,*], Suharso[a,*], Mita Rilyanti[a], Miranda Sari[a], Sumadi[b]

[a]*Department of Chemistry, Faculty of Mathematic and Natural Sciences, University of Lampung, Bandar Lampung 35145, Indonesia, Tel. +62(721)-7625088; Fax: +62(721)-704625; emails: buhani_s@yahoo.co.id (Buhani), suharso_s@yahoo.com (Suharso)*
[b]*Department of Electrical Engineering, Faculty of Engineering, University of Lampung, Bandar Lampung 35145, Indonesia*

Received 28 May 2020; Accepted 22 December 2020

ABSTRACT

Modification of palm oil shells carbon coated by Fe_3O_4 (magnetite) particle (PPAC-PMnPs) as adsorbent to remove Cd(II) ions from solution was investigated using batch method. The palm oil shells carbon activated (PPAC-P) and PPAC-PMnPs adsorbent were identified by several instruments as infrared (IR) spectrometer to identify the functional groups, SEM-EDX (scanning electron microscope and energy dispersive X-ray spectroscopy) to investigate element constituents and surface morphology, Brunauer–Emmett–Teller analyzer to determine surface areas, and X-ray diffraction to analyze crystallization level of the adsorbents. Identification of Cd(II) ion concentrations in the solutions of experiments was determined by an atomic absorption spectrometer. The adsorption process of Cd(II) ion by the PPAC-P and PPAC-PMnPs adsorbents was optimum at pH 6 and 7 with a contact time of 90 min. The adsorption kinetics of Cd(II) ions on PPAC-P and PPAC-MnPs has a tendency to follow the pseudo-second-order kinetics model and Freundlich adsorption isotherm model with a correlation coefficient (R^2) >0.99. These facts show that adsorption process between the Cd(II) ion and PPAC or PPAC-PMnPs adsorbent runs as heterogeneous adsorption. The PPAC-PMnPs adsorbent can be used repeatedly with % Cd(II) ion adsorbed almost constant for four repetition cycles with absorption efficiency >80%.

Keywords: Modified carbon; Palm oil shells; Magnetite coating; Cd(II) ion adsorption

1. Introduction

Pollution due to heavy metals in the surroundings from increased activity in technology and industry is a global problem, and the appearance of metals that are categorized as poisonous in various waters poses a danger to the development of ecological and economic systems [1]. Cadmium (Cd) is a toxic element that is often found in industry used as a pigment material, stabilizer of plastic synthesis, Ni-Cd battery, metal coating, and alloy [2,3].

Several experiments were studied for wastewater treatment that contains toxic chemicals such as adsorption, chemical precipitation, coagulation, electro dialysis, ultrafiltration, reverse osmosis, flotation, and ion exchange [4]. From the several methods available today, adsorption is one method that is quite widely used because this method is easy, relatively cheap, and environmentally friendly [5,6]. Success of the adsorption technique is principally decided by compatibility of nature and type of adsorbent applied. The adsorption effectivity from adsorbents is

---

* Corresponding authors.

determined by high adsorption capacity, reused for several times, chemically stable, friendly to the environment [7,8].

Activated carbon (AC) is one of the most effective matter applied as adsorbent in adsorbing metal ions in solution. Until now, various carbon-based adsorbent materials have been successfully used in the removal of different pollutant types such as heavy metal ions [9], surfactants [10] and dyes [11] from water. The increasing use of activated carbon fosters creativity to maximize the function of carbon, not only from the surface area and its pores but also on the carbon surface as well. The ability of AC adsorption is determined by its structure and surface chemistry.

The activated carbon holds benefits as an adsorbent in several sides, but it possess limitedness in segregation of the activated carbon remaining side products and regeneration for reused [7]. Consequently, the improvement of the quality of AC, among others by providing magnetic characteristics to the AC via the superparamagnetic particle coating technique of Fe_3O_4 is necessary. The coating technique with Fe_3O_4 will produce AC that is stable under acidic conditions [12]. In addition, at room temperature there are magnetic properties in AC that can separate adsorbate quickly [13]. Use of magnetite particles for coating material is a technique which is environmentally friendly because this technique does not produce contamination products as suspended solids, in addition to accelerating the process of isolating metals in solution because adsorbents are magnetic [14–17]. In general, centrifugation and filtration methods are used to separate the adsorbent material from aqueous solution [11]. These applications are time-consuming and require extra cost [18]. Compared with traditional centrifugation and filtration methods, magnetic separation method is an efficient, fast and economic method for the separation of magnetic adsorbents from the medium after the adsorption treatment of pollutants is completed [19].

The adsorbents modified by magnetic coating may be isolated from the solution system with using an external magnet. Most magnetic adsorbents use Fe_3O_4 particles because it is known that the magnetite phase has good magnetic properties [18,20]. Combining AC with magnetite is a promising method for removing metal ions. Cations will be electrostatically attracted to the magnets that are in the pores of the AC, causing a fairly large adsorption power [13]. The cations will be adsorbed through surface complexation, chemisorption, and co-precipitation [21]. Moreover, cations were able to be bonded and attracted via hydrogen bonding, ion exchange, chemisorption, and complexation (chelation) [22]. In this research, the production of AC-magnetite (PPAC-PMnPs) was carried out from physically activated palm oil shells (PPAC-P) and its application as adsorbent of Cd(II) ion in aqueous solution. The development of adsorbents from AC-magnetite can increase the adsorbents ability to remove Cd(II) ions efficiently compared with other adsorbents. Various adsorption parameters studied will be used as a model to optimize the use of AC from oil palm shells so that they can provide useful information for effective and inexpensive wastewater treatment.

2. Experimental procedure

2.1. Materials

Palm oil shells applied for current work came from waste treatment of palm oil in Province of Lampung (Indonesia). The chemicals used in this study were $FeSO_4·7H_2O$, $FeCl_3·6H_2O$, $Cd(CH_3COO)_2·2H_2O$, $NaNO_3$, NaOH, NH_4OH, and HCl. All chemicals applied in this work are of AR grade from European Pharmacopoeia, France.

2.2. Preparation of PPAC-PMnPs adsorbent

Palm oil shells are cleaned and dried in the sun. The palm oil shells that have been cleaned were carbonized by burning them in drums made of special iron plates for about 6 h to obtain carbon. The carbon obtained was crushed using a grinding device and then sifted with a 100 micron sieve. Furthermore, the carbon was physically activated by burning 200 g of carbon in a furnace at 700°C for 1 h. Then it was cooled in a desiccator until the temperature was stable, followed by a separation between the activated carbon and the ash formed, so that physically activated carbon (PPAC-P) was obtained.

Production of PPAC-PMnPs adsorbent was made with reacting 7.60 g of $FeCl_3·6H_2O$ and 3.9 g of $FeSO_4·7H_2O$ were dissolved into distilled water (300 mL) at temperature 60°C. Then 6.5 g of PPAC-P were mixed in the solution. The admixture obtained was mixed for 30 min while adding 100 mL of 5 M NaOH dropwise to form a black precipitate. The resulting precipitate was filtered and washed by water distilled until it was neutral and continued by drying at 100°C in an oven for 3 h to obtain PPAC-PMnPs adsorbent [7].

2.3. Characterization of PPAC-PMnPs

The PPAC-PMnPs were observed with using infrared spectrometer (FTIR) to investigate the existence of specific functional groups contained inside the material (Prestige-21 Shimadzu, Japan). Characterization by X-ray diffraction was performed to determine the mineral phases (Shimadzu 6000, Japan). The morphology of surface and elements of constituent from the substance was investigated with using instrument made in Germany (Zeiss MA10, SEM-EDX, Gottingen, Germany). The surface analyzer (Quantachrome Instrument made in USA, TouchWin v1.0) was used to measure the specific surface area and pore size of materials. The pH_{PZC} called point of zero charge to PPAC-P and PPAC-PMnPs was measured by method of the pH drift.

2.4. Measurement of pH_{PZC} (zero point charge) of PPAC-PMnPs

The zero point charge was measured using 0.01 M $NaNO_3$ aqueous solutions in pH of 2–9. The values of current pH were constant with either a NaOH (0.1 M) or HCl (0.1 M) watery solution. Each (5 mL from these solutions) was mixed with the sample (0.01 g) and continued with a stirring of the system for 48 h [23]. The pH of the supernatant decanted was measured. The values of the

pH_{PZC} were resulted through plotting the pH from initial solution vs. the pH of supernatant.

2.5. Adsorption experiment

A stock of Cd(II) ion solution (1 g L^{-1}) was first made with dissolving $Cd(CH_3COO)_2{\cdot}2H_2O$ in water deionized. All working solution at desired concentration were made from the stock solution obtained with diluting by water deionized. The sorption behavior from Cd(II) ions on the PPAC-PMnPs was investigated using the Cd(II) ion aqueous solutions. An amount of 0.1 M NaOH or 0.1 M HCl was used to arrange the initial pH. The experiments of adsorption using batch method were performed in various parameters which cover solution pH, contact time, and Cd(II) ion concentration. To complete this, under ambient conditions, the PPAC-PMnPs (0.05 g) was immersed and mixed into solution of Cd(II) ions (25 mL). The solution pH, contact time, and Cd(II) ion concentration were varied from 3.0 to 9.0, 15 to 120 min, and 25 to 300 mg L^{-1}, successively. The concentrations of Cd(II) ions were calculated using instrument of atomic absorption spectrometer (Agilent 24 Series AA, Australia).

The amount of adsorbed Cd(II) ion by mass unit of adsorbent material together with the bonded Cd(II) ion percentage was calculated by Eqs. (1) and (2), successively:

$$q_e = \frac{\left(C_0 - C_e\right)v}{w} \tag{1}$$

$$\text{Adsorption}\left(\%\right) = \frac{\left(C_0 - C_e\right)}{C_0} \times 100 \tag{2}$$

with C_e and C_0 in mg L^{-1} are Cd(II) ion concentration after and before process of adsorption, w is mass for adsorbent in g, q_e is total of bonded Cd(II) ions by mass unit (mg g^{-1}), and v is volume of solution in L.

The obtained data from the adsorption process were investigated by determining the correlation between the total of adsorbed Cd(II) ions in solution experimentally and estimation results applying adsorption isotherm equations of Langmuir and Freundlich. The evaluation was carried out by determining RMSE (root mean squared error) Eq. (3) and χ^2 (Chi-square test) Eq. (4) [24,25], respectively:

$$\text{RMSE} = \sqrt{\left(\frac{1}{m-2}\right)\sum_{i=1}^{m}\left(q_{i,\text{exp}} - q_{i,\text{cal}}\right)^2} \tag{3}$$

$$\chi^2 = \sum_{i=1}^{m} \frac{\left(q_{i,\text{exp}} - q_{i,\text{cal}}\right)^2}{q_{i,\text{exp}}} \tag{4}$$

with $q_{i,\text{exp}}$ and $q_{i,\text{cal}}$ are each gained from the experimental and estimate results through the adsorption isotherm equation, m is total of observations in experiment of sorption. The RMSE with smaller value describes well curve fitting, in addition if the resulted data by the pattern are near to the results of the experiment, χ^2 may be small number [24,26].

3. Results and discussion

3.1. Characterization of PPAC-PMnPs adsorbent

The PPAC-PMnPs material characterizations were performed by FTIR spectroscopy, X-ray diffraction (XRD), SEM-EDX, and BET analyzer. In Fig. 1, it can be observed that in PPAC-P and PPAC-PMnPs, there is the same absorption in the area of about 3,500 cm^{-1}, which shows the existence of stretching vibration from the hydroxyl group (O–H) [27]. The absorption bands of the wave numbers that appear in PPAC-P and PPAC-PMnPs are 2,360.56 and 2,368.56 cm^{-1}, respectively (Figs. 1b and c) showing a stretching vibrations of C–C [28]. In PPAC-PMnPs, the absorption band appears at wave number 586.36 cm^{-1} (Fig. 1b), which is a typical absorption of Fe–O (Fig. 1a) [29]. This shows that the magnetite coating on PPAC-P has been successfully carried out.

In Fig. 2, it can be seen X-ray diffraction (XRD) patterns of PPAC-P and PPAC-PMnPs compared with magnetite. On the PPAC-P diffractogram (Fig. 2b), it shows an amorphous carbon phase, this is commonly found in activated carbon, where the peak is widening at 25°–35° [13,30]. Whereas in PPAC-PMnPs (Fig. 2c), the diffractogram, which was initially sloping became flat and new peaks appeared in the 2θ area, respectively, at 30.09°, 35.53°, 43.08°, 56.96°, and 62.49°. The XRD pattern on PPAC-PMnPs indicates a modification in the alleviation of the amorphous carbon to the crystalline phase [31,32] as found in the magnetite diffraction pattern (Fig. 2a). This clearly demonstrates that magnetite particles are successfully embedded in the framework of PPAC-P.

The isotherms of N_2 adsorption–desorption with the curves of pore size distribution of PPAC-P and PPAC-PMnPs are investigated in Fig. 3a and they describe a trend to comply the scheme of the isotherm of the adsorption–desorption of the merged adsorption isotherm of type I and IV. The type 1 adsorption isotherm only shapes one layer on adsorbate and it happens by chemisorption mechanism. The adsorption isotherm model of type IV take places in the taller P/Po zone by hysteresis loop of model

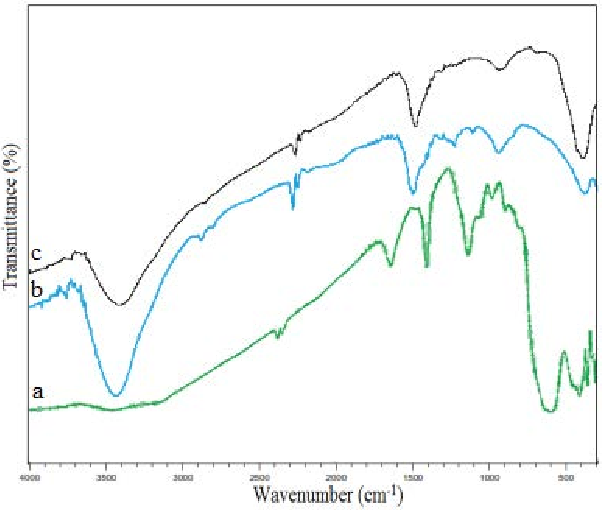

Fig. 1. Infrared spectra of (a) magnetite, (b) PPAC-P, and (c) PPAC-PMnPs.

H1 proving mesoporous adsorbent [31]. The pore size distribution of PPAC-PMnPs originated of the adsorption branch from isotherm process indicates the greatly possible pore size concentrated at 3.22 nm (Fig. 3b). BET for surface area and pore volume of the obtained PPAC-P are 416.13 m^2 g^{-1} and 0.23 cm^3 g^{-1}, successively. After introducing magnetite particles, the surface area of BET and volume of pore from PPAC-PMnPs decreases significantly to 300.09 m^2 g^{-1} and 0.21 cm^3 g^{-1}, respectively, which is lower than that of the PPAC-P. As contrasted to BET for the surface area and total pore volume, PPAC-P and PPAC-PMnPs, they indicate that the structure of PPAC-PMnPs does not alter with by addition of magnetite particles that promote that the material of PPAC-PMnPs is still controlled by PPAC-P. In addition, the magnetite particles coating on PPAC-P conduces a lowering on the surface region and pore volume on the PPAC-PMnPs.

Figure of SEM of the surface morphology from the PPAC-P and PPAC-PMnPs is displayed in Fig. 4. On the PPAC-P, it was found the uniform pores (Fig. 4a) then since coating magnetite particles, it was obtained a lowering at the amount of pores on material of PPAC-PMnPs (Fig. 4b). Pore degradation in PPAC-PMnPs is because of important pore obstacle by the magnetite particles coating [13,31]. Analysis with EDX support the data obtained, which indicate that in material of PPAC-PMnPs, in addition, the existence of O and C elements, which are constituent elements of adsorbent of PPAC-P (Fig. 4c), the existence of Fe element is found also as an element come from particle of magnetite (Fig. 4d). Fig. 4c describes the analysis of EDX for PPAC-P. The emerged peaks coressponding to O and C are indicated as the only elements.

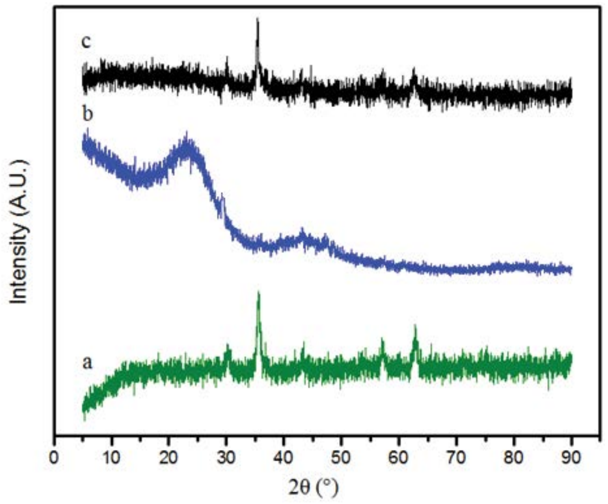

Fig. 2. X-ray diffraction patterns of (a) magnetite, (b) PPAC-P, and (c) PPAC-PMnPs.

3.2. Influence of pH

Solution pH is believed as the greatly significant environmental elements to allow in evaluating the value of main application of an adsorbent since it effects on material surface charge, its adsorption capacity, and heavy metal ions types existed in aqueous solution. Initial pH effect on sorption of Cd(II) ions on PPAC-P and PPAC-PMnPs was studied at acidic, neutral, and basic pH (pH 3.0–9.0) (Fig. 5a).

In general, the pH optimum on the sorption of Cd(II) ions is at pH 6.0 on PPAC-P and pH 7.0 on PPAC-PMnPS (Fig. 5a). The point where the zeta potential is nil is named the zero charge point (pH$_{PZC}$), which is applied to values of the surface charge. The positive of the surface charge occurs at pH < pH$_{PZC}$, while the negative of the surface charge occurs at pH > pH$_{PZC}$. In this situation, the solid addition method determines the pH$_{PZC}$ of the PPAC-P and PPAC-PMnPs (Fig. 5b) at around 6.0 and 6.5, respectively. As the pH$_{PZC}$ is above the solution pH, the PPAC-MnPs obtain a positive surface charge. The effects of competition on the electrostatic repulsion and ions of H$^+$ between the positively charged active adsorption sites on the PPAC-PMnPs and ions of Cd(II) could produce a lowering in the adsorption capacity of Cd(II) ions. As pH$_{PZC}$ < pH, the negative surface charge on the material of the PPAC-P and PPAC-PMnPs indicates a necessary electrostatic attraction upon the species of the Cd(II) ion positive charges in the watery solutions. Raised pH raises the interactions of

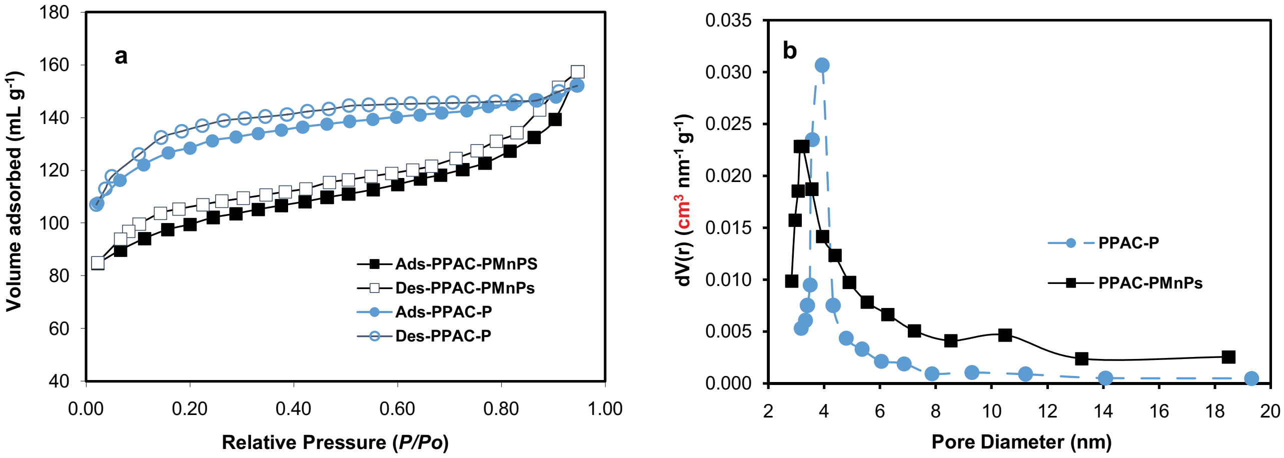

Fig. 3. (a) N$_2$ adsorption/desorption isotherms and (b) pore size distribution of PPAC-P and PPAC-PMnPs.

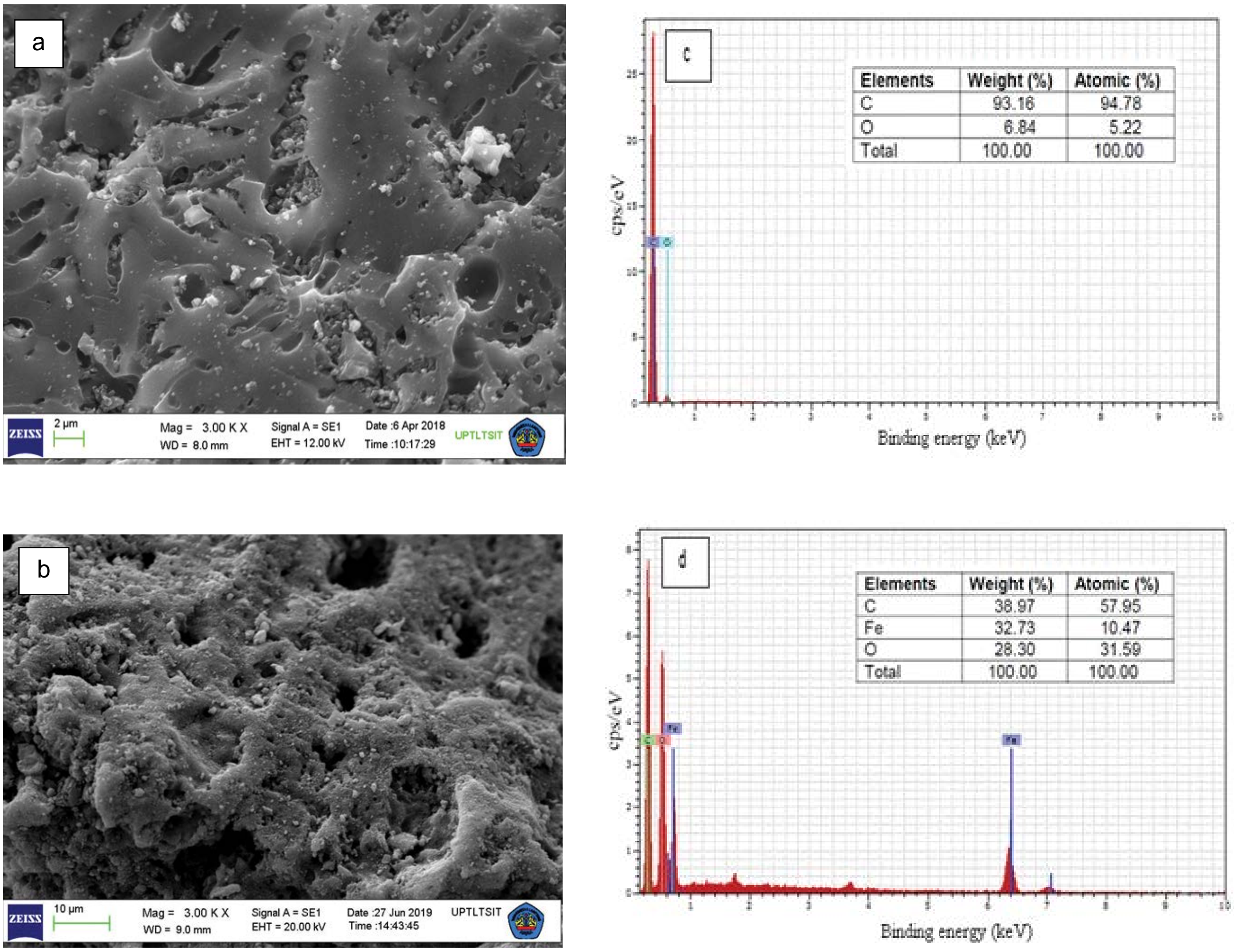

Elements	Weight (%)	Atomic (%)
C	93.16	94.78
O	6.84	5.22
Total	100.00	100.00

Elements	Weight (%)	Atomic (%)
C	38.97	57.95
Fe	32.73	10.47
O	28.30	31.59
Total	100.00	100.00

Fig. 4. SEM images and EDX spectra of (a), (c) PPAC-P and (b), (d) PPAC-PMnPs.

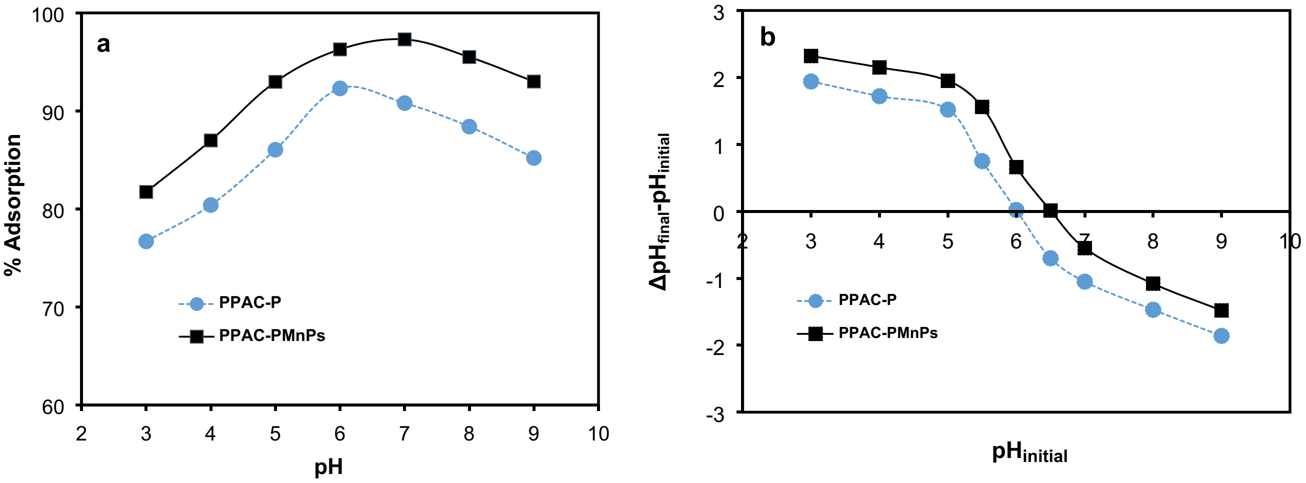

Fig. 5. (a) Influence of pH on Cd(II) ions adsorption to PPAC-P and PPAC-PMnPs and (b) determination of the point of zero charge (pH_{PZC}) of the PPAC-P and PPAC-PMnPs.

electrostatic force between Cd(II) ions and the surface active sites, which are negative charge of PPAC-P and PPAC-PMnPs. At pH higher than 7, the sorption process starts to decrease since Cd(II) ion tends to hydrolyze to form a hydroxyl ions species precipitating [32,33]. Moreover, at these conditions, the material surface becomes negatively charged resulting in repulsion force between the material surface and metal ions species. Finally, the adsorption process will be decreasing.

The percentage of Cd(II) ion adsorbed in PPAC-PMnPs is bigger than PPAC-P, this happens because of the rise of active sites and the magnetic characteristic of the material resulted by the existence of the magnetic particle [31]. This indicated that the surface charges of both PPAC-P and PPAC-PMnPs change, as a function of pH to present a main role on the sorption process.

3.3. Contact time

One of the important optimization parameters on the sorption process is the contact time, because it can provide information about the duration of the adsorption time to absorb or eliminate the targeted adsorbate maximally in aqueous media. The adsorption contact time data can be used to observe the time of equilibrium at a peak adsorbate absorption and to determine the adsorption process kinetics. At this work, the influence of contact time from Cd(II) ions on adsorbents of PPAC-P and PPAC-PMnPs was investigated in the range of 15–120 min displayed in Fig. 6.

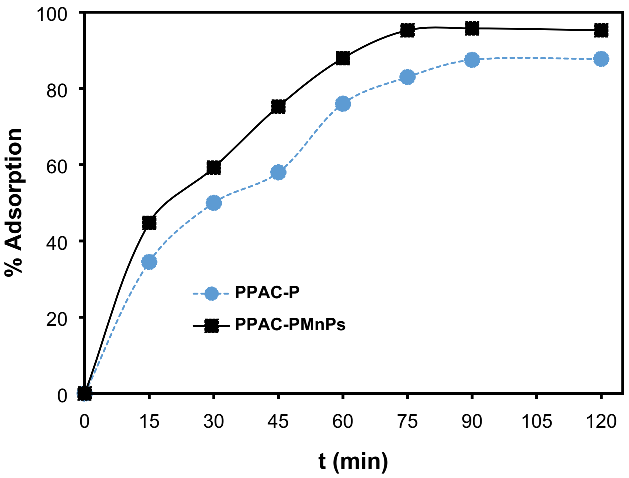

Fig. 6. Influence of contact time on adsorption of Cd(II) ions onto PPAC-P and PPAC-PMnPs.

Fig. 6 shows that the maximum adsorption from Cd(II) ions by PPAC-P and PPAC-PMnPs around 90 min and increasing contact time to 120 min does not significantly increase the absorption of Cd(II) ions in both adsorbents. Therefore, it could be expressed that the process of adsorption has achieved an equilibrium at this level [34].

The kinetic model of the sorption process for Cd(II) ions in the solution adsorbed on PPAC-P and PPAC-PMnPs was determined by analyzing the data contained in Fig. 6 using Eq. (5) for pseudo-first-order and Eq. (6) for pseudo-second-order [28,35] as follows:

$$\log\left(q_e - q_t\right) = \log q_e - \frac{k_1}{2.303}t \tag{5}$$

$$\frac{t}{q_t} = \frac{1}{k_2 q_e^2} + \frac{t}{q_e} \tag{6}$$

where q_e is an amount of adsorption capacity from Cd(II) ions at equilibrium time in mg g^{-1} and q_t is an amount of adsorption capacity from Cd(II) ions at time of t (mg g^{-1}). While k_1 (min^{-1}) and k_2 (g mg^{-1} min^{-1}) belong to the first and second order rate constants, successively. Adsorption kinetics parameters such as adsorption rate constants and Cd(II) ion regression coefficients in PPAC-P and PPAC-PMnPs may be seen from Table 1.

Table 1 describes a correlation coefficient (R^2) to kinetic pattern of the pseudo-second-order in PPAC-P and PPAC-PMnPs with the values of 0.982 and 0.993, serially, the value is relatively greater than the kinetic model from the pseudo-first-order (R^2 = 0.839 and 0.931). These data indicate that the kinetic model of sorption of Cd(II) ions in solution in the two adsorbents derived from oil palm shells tends to attend the pseudo-second-order kinetics model. This indicates that the Cd(II) ions sorption by PPAC-PMnPs not only occurs through physical adsorption but there is a contribution of chemical adsorption through the group activities of the adsorbent [36,37]. In literature, similar kinetic results were reported for the adsorption of various water pollutants by organic [38] and inorganic [39] adsorbents. In addition, it could also be observed that the sorption rate (k_2) of Cd(II) ions by PPAC-PMnPs was greater than that of PPAC-P. This occurs because of the magnetic properties of PPAC-PMnPs derived from magnetite particles, which can increase the rate of adsorption of Cd(II) ions in solution to PPAC-PMnPs [40].

The mechanism of sorption is greatly contingent on adsorbent surface specific used and an adsorbate being interacted [41,42]. To investigate the sorption mechanism of Cd(II) ions on PPAC-P and PPAC-PMnPs, data

Table 1
Adsorption kinetic parameter for the adsorption of Cd(II) ions on PPAC-P and PPAC-PMnPs

Adsorbents	Pseudo-first-order		Pseudo-second-order	
	k_1 (min^{-1})	R^2	$k_2 \times 10^{-4}$ (g mg^{-1} min^{-1})	R^2
PPAC-P	0.071	0.839	8.240	0.982
PPAC-PMnPs	0.110	0.931	40.640	0.993

analysis was done using equation made by Weber and Morris (intra-particle diffusion model) Eq. (7) [34,43]. This model is widely used to investigate the diffusion process of targets absorbed by adsorbents that can be used in simulating kinetics data [44].

$$q_t = k_{\text{id}} t^{0.5} + C \tag{7}$$

with k_{id} in mg g^{-1} min$^{-0.5}$ belongs to a rate constant of intra-particle diffusion, and the value of C in unit of mg g^{-1} belongs to a constant depicting resistance for transfer of mass in the border layer. They were identified based on the intercept and slope of lines gained by plotting q_t against $t^{0.5}$. The values of the C and k_{id} are investigated from intercepts and slope in Fig. 7 and the C and k_{id} values are shown in Table 2.

The diffusion of intra-particle can be gained from the plots of q_t against $t^{0.5}$. When it produces a linear line, accordingly, it becomes stage of rate limiting causing film diffusion drive the process of adsorption [45]. In Fig. 8 it can be seen that two linear parts occur for every the plot. These model give indication that the model of the adsorption process involved more than one. Transfer of external mass is indicated by the premier linear portion with the sorption interval range from 0 to 60 min. The diffusion of intra-particle is represented by the secondly linear portion with the sorption interval range from 60 to 120 min. The secondly linear portion is not over the source (C ≠ 0), proving that the intra-particle diffusion occurs not only by the step of rate controlling but also the transfer of the external mass involves simultaneously [43].

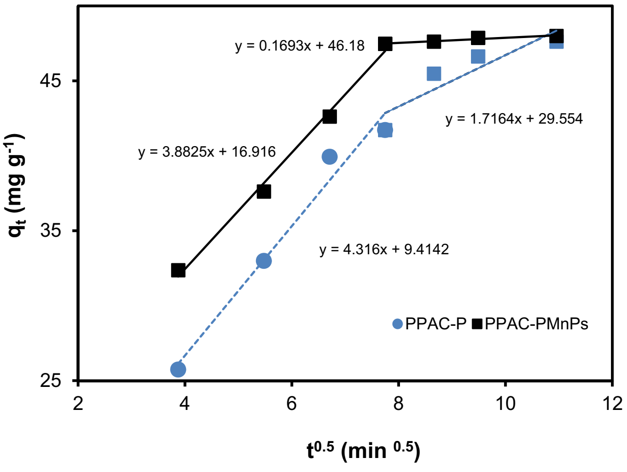

Fig. 7. Intra-particle diffusion (IPD) model predicted kinetics of Cd(II) ions sorption by PPAC-P and PPAC-PMnPs.

According to the corresponding data in Fig. 7, both models great describe the Cd(II) ion transfer between solution and the PPAC-PMnPs external face continued with the next directional diffusion of the ions of target for the binding sites via area of pores, successively, based on the theory of adsorption–diffusion generally. In Fig. 7, the slopes of the second step describing diffusion rate occur only rather down than the slope of the first step. This indicates that in pore area the directional diffusion of Cd(II) ions is not significantly slow.

3.4. Adsorption isotherm

The patterns of PPAC-P and PPAC-PMnPs adsorption isotherms in absorbing Cd(II) ions in watery solution were explored by interacting a solution of Cd(II) ions at various concentrations started from 0 to 300 mg L^{-1}. Fig. 8 describes the Cd(II) ion adsorption, which rises harshly at lower equilibrium concentrations continued with slowly rise when the concentrations is higher, indicating that both PPAC-P and PPAC-PMnPs have a high adsorption affinity for Cd(II) ions.

The sorption isotherms (Fig. 8) can be employed to explore the interactions between Cd(II) ions and adsorbent. The data obtained from the experiment were tested by the isotherm patterns from the equations of the Langmuir and Freundlich as pointed in Eqs. (8) and (9) serially. The sorption isotherm of the Langmuir assumes that each site of adsorption and potency of binding from adsorbate can be similar and not dependent whether the neighboring sites can be placed or free. This statement describes that the adsorption happens to shape a monolayer on the face of the substrate and the sorption energy has been distributed equally on the whole surface [46,47].

$$\frac{C_e}{q_e} = \frac{1}{q_m K_L} + \frac{C_e}{q_m} \tag{8}$$

where in q_e in unit of mg g^{-1} is total of adsorbed Cd(II) ions by unit weight of adsorbent and C_e in unit of mg L^{-1} is an adsorbate concentration, which is unadsorbed at equilibrium in solution. The constant of Langmuir is stated as constant of K_L (L mg^{-1}) and the maximal monolayer sorption potency is written as q_m (mg g^{-1}). The plot C_e/q_e against C_e produces an intercept and slope, $1/q_mK_L$ and $1/q_m$ successively.

The equation that describes the interaction of adsorption on heterogeneous surfaces with active sites that have non-uniform energy and adsorption on multilayers can be

Table 2
Intra particle diffusion model for Cd(II) ions on PPAC-P and PPAC-PMnPs

Adsorbent	Initial linear portion			Second linear portion		
	k_{i1} (mg g^{-1} min$^{-0.5}$)	C_1 (mg g^{-1})	R_1^2	k_{i2} (mg g^{-1} min$^{-0.5}$)	C_2 (mg g^{-1})	R_2^2
PPAC-P	4.316	9.414	0.975	1.716	29.554	0.821
PPAC-PMnPs	3.882	16.916	0.993	0.169	46.180	0.942

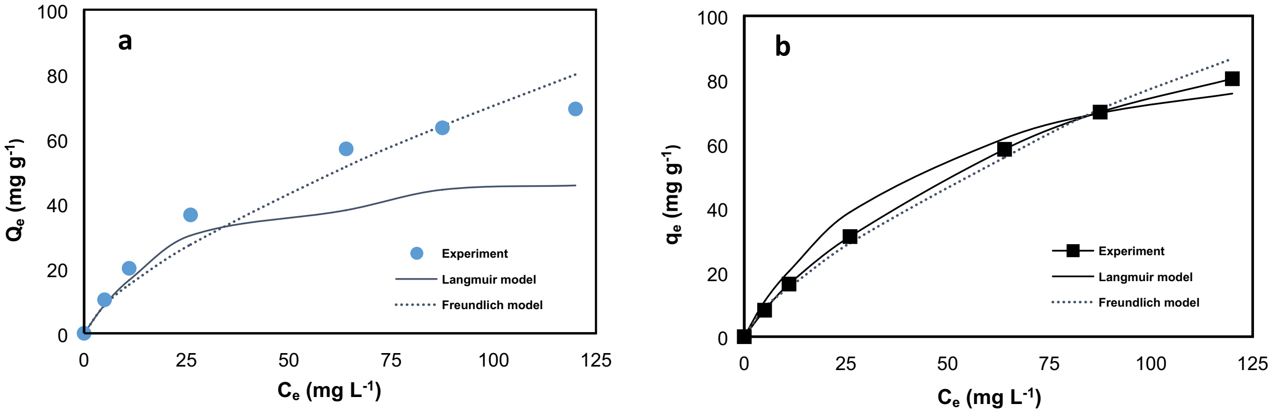

Fig. 8. Adsorption isotherm model of Cd(II) ions on (a) PPAC-P and (b) PPAC-PMnPs.

understood by the Freundlich model [48] and represented by Eq. (9).

$$\log q_e = \log K_F + \frac{1}{n}\log C_e \tag{9}$$

where n is the factor of sorption intensity (1–10) and K_F is a factor of adsorption capacity with the unit of (mg g^{-1}) (L mg^{-1})$^{1/n}$ [49]. Next, with plotting of logC_e against log q_e produces K_F and model of exponent n is exclusively used to explain the adsorption of multilayer on surfaces, which are heterogeneous.

The relevant parameters and the linear fit to the model of Freundlich are displayed in Table 3 and Fig. 8, successively. As illustrated in Table 3, in Freundlich adsorption isotherm model, the correlation coefficients performed the Freundlich model ($R^2 > 0.99$), RMSE and χ^2 values are smaller than in adsorption isotherm of Langmuir. This suggests that Cd(II) ions adsorption mechanism on the adsorbent of PPAC-P and PPAC-PMnPs is classified as heterogeneous adsorption. This denotes that the Cd(II) ion adsorption on the adsorbent of PPAC-P and PPAC-PMnPs occurs via the active carbon pores and classified as physical interactions. Similar results were reported for the adsorption isotherms of various adsorbent-pollutant systems in literature [50–52].

Table 3
Langmuir and Freundlich parameters for the adsorption of Cd(II) ions on PPAC-P and PPAC-PMnPs

Adsorbent		PPAC-P	PPAC-PMnPs
Models	Parameters		
	q_{exp} (mg g^{-1})	69.332	80.400
Langmuir			
	q_m (mg g^{-1})	92.131	104.074
	$K_L \times 10^{-4}$ (L mg^{-1})	8.197	9.259
	R^2	0.852	0.819
	RMSE	3.599	4.363
	χ^2	3.895	4.203
Freundlich			
	K_F (mg g^{-1}) (L mg^{-1})$^{1/n}$	2.802	3.114
	n	1.430	1.382
	R^2	0.994	0.995
	RMSE	3.211	2.735
	χ^2	1.232	0.896

Fig. 8 describes that the Cd(II) ion concentration adsorbed in PPAC-PMnPs is relatively more than in PPAC-P adsorbents. This occurs because in PPAC-PMnPs there are activated carbon pores and the presence of material magnetic properties of magnetite particles, which can increase the rate and capacity of adsorption [53]. The concentrations of adsorbed Cd(II) ion were identified through the results of experiment (q_{exp}) on PPAC-P and PPAC-PMnPs with the value of 69.332 and 80.400 mg g^{-1}, serially (Table 3).

The data obtained to the capacity of adsorption (q_{exp}) from this research can be contrasted by other adsorbents of Cd(II) ion (Table 4). From the comparison of data obtained, the PPAC-PMnPs material is one of the well materials to bind the Cd(II) ions in watery solution, specifically in processing of Cd heavy metal waste.

3.5. Reuse of adsorbents

The regeneration and reusability of an absorbent were most significant features for the practical application. To be profitable in the adsorption process, the adsorbent used must be able to be used repeatedly to reduce the amount of material costs and the adsorbed metal ions must be easily adsorbed under appropriate conditions. The capability to reuse PPAC-P and PPAC-PMnPs adsorbent in the Cd(II) ion solution was investigated by the Cd(II) ion adsorption for five repetitions described in Fig. 9. The adsorption was performed by interaction of PPAC-P and PPAC-PMnPs with Cd(II) ion solution at pH optimum (pH 6 for PPAC-P and pH 7 for PPAC-PMnPs), contact time (90 min), and 27°C. Desorption of adsorbed Cd(II) ions on the adsorbent was eluted applying 0.1 M hydrochloric acid solution. The adsorbent regeneration was cleaned by aquadest to be the pH with neutral condition, dried in 60°C for 24 h, and reapplied for recurrent

Table 4
Adsorption capacity of Cd(II) ions on PPAC-PMnPs compared with other adsorbents

Adsorbent	q_m (mg g^{-1})	Experimental condition (pH; equilibrium time [min]; and temperature [°C])	Reference
Cd(II) ion-imprinted ionic polymer	83.89	6.0, 60, 27	[3]
Nannochloropsis sp.-silica	23.81	5.0, 60, 27	[54]
Urea-modified wheat straw	39.22	6.0, 20, 30	[55]
Olive stone activated carbon	11.72	5.0, 7, 25	[56]
Mercapto-modified graphene oxide	36.00	5.0, 20, 25	[57]
Carboxyl-modified jute fiber	88.98	6.0, 20, 25	[58]
Cellulose nanofibers	45.90	4.0, 600, 25	[59]
Iron-trimesic metal–organic frameworks	54.95	5.0, 20, 25	[60]
PPAC-PMnPs	80.40	7.0, 90, 27	This work

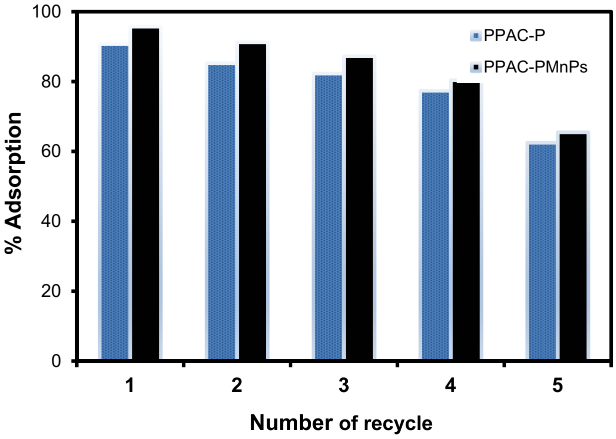

Fig. 9. Reusability number efficiency of the adsorption–desorption process of of Cd(II) ions on PPAC-P and PPAC-PMnPs.

sorption. The use of HCl as an eluting agent is because in an acidic medium, the active group in the adsorbent containing hydrogen will be protonated and does not attract cations, resulting in the release of cations into the eluent solution or desorption agent [61].

The percentage of Cd(II) ions adsorbed on PPAC-PMnPs was nearly stable to the first four cycles by absorption efficiency >80%. For the fifth cycle, the adsorption efficiency has begun to decrease because the washing process of adsorbent during the desorption process affects the surface properties so that it damages the active adsorbent site. From the results of this study, it can be stated that PPAC-MnP adsorbents can function as economical and effective adsorbents for removing Cd(II) ions in solution.

4. Conclusions

Magnetite coating on activated carbon modification derived from oil palm shells was performed effectively and may be applied as adsorbent of Cd(II) ions in watery solution. The pH optimum for sorption of Cd(II) ions on PPAC-PMnPS occurs at pH 7.0. The sorption mechanism tends to attend the adsorption isotherm kinetics model of pseudo-second-order and Freundlich. The rate and capacity of sorption of Cd(II) ions adsorbed on PPAC-PMnPs is greater than PPAC-P. The PPAC-PMnP adsorbents can be used repeatedly in the process of adsorption–desorption and the percentage of Cd(II) ions adsorbed is almost constant for the first four cycles with adsorption efficiency >80%. Thus the PPAC-PMnPs are effective and good adsorbents for removing heavy metals specifically Cd(II) ion in solution.

Acknowledgments

This research was sponsored by Ministry of Research and Technology/Institute of Research and National Innovation of the Republic of Indonesia with contract number: 179/SP2H/AMD/LT/DPRM/2020. The authors would also like to thank Technical Service Unit of the Integrated Laboratory and the Technology Innovation Center–University of Lampung (UPT Laboratorium Terpadu dan Sentra Inovasi Teknologi–Universitas Lampung) for the assistance of the devices applied in this project.

References

[1] H. Zou, E. Hu, S. Yang, L. Gong, F. He, Chromium(VI) removal by mechanochemically a sulfidated zero valent iron and its effect on dechlorination of trichloroethene as a co-contaminant, Sci. Total Environ., 650 (2019) 419–426.
[2] M.J. Scoullos, G.H. Vonkeman, I. Thornton, Z. Makuch, Mercury-Cadmium-Lead: Handbook for Sustainable Heavy Metals Policy and Regulation, Kluwer Academic Publishers, Dordrecht, the Netherlands, 2001.
[3] Buhani, Narsito, Nuryono, E.S. Kunarti, Production of metal ion imprinted polymer from mercapto-silica through sol-gel process as selective adsorbent of cadmium, Desalination, 251 (2010) 83–89.
[4] I. Ali, V.K. Gupta, Advances in water treatment by adsorption technology, Nat. Protoc., 1 (2007) 2661–2667.
[5] Buhani, Musrifatun, D.S. Pratama, Suharso, Rinawati, Modification of *Chaetoceros* sp. biomass with silica-magnetite coating and adsorption studies towards Cu(II) ions in single and binary system, Asian J. Chem., 29 (2017) 2734–2738.
[6] V. Kårelid, G. Larsson, B. Björlenius, Pilot-scale removal of pharmaceuticals in municipal wastewater: comparison of granular and powdered activated carbon treatment at three wastewater treatment plants, J. Environ. Manage., 193 (2017) 491–502.
[7] Buhani, F. Hariyanti, Suharso, Rinawati, Sumadi, Magnetized algae-silica hybrid from *Porphyridium* sp. biomass with Fe_3O_4 particle and its application as adsorbent for the removal of

methylene blue from aqueous solution, Desal. Water Treat., 142 (2019) 331–340.

[8] U.A. Guler, M. Sarioglu, Mono and binary component biosorption of Cu(II), Ni(II), and methylene blue onto raw and pretreated *S. cerevisiae*: equilibrium and kinetics, Desal. Water Treat., 52 (2014) 4871–4888.

[9] O. Duman, E. Ayranci, Attachment of benzo-crown ethers onto activated carbon cloth to enhance the removal of chromium, cobalt and nickel ions from aqueous solutions by adsorption, J. Hazard. Mater., 176 (2010) 231–238.

[10] O. Duman, E. Ayranci, Adsorptive removal of cationic surfactants from aqueous solutions onto high-area activated carbon cloth monitored by in situ UV spectroscopy, J. Hazard. Mater., 174 (2010) 359–367.

[11] O. Duman, S. Tunç, B.K. Bozoglan, T.G. Polat, Removal of triphenylmethane and reactive azo dyes from aqueous solution by magnetic carbon nanotube-κ-carrageenan-Fe_3O_4 nanocomposite, J. Alloys Compd., 687 (2016) 370–383.

[12] L. Qimeng, Q. Yanshan, G. Canzhu, Chemical regeneration of spent powdered activated carbon used in decolorization of sodium salicylate for the pharmaceutical industry, J. Cleaner Prod., 86 (2015) 424–431.

[13] K.T. Wong, N.C. Eu, S. Ibrahim, H. Kim, Y. Yoon, M. Jang, Recyclable magnetite-loaded palm shell-waste based activated carbon for the effective removal of methylene blue from aqueous solution, J. Cleaner Prod., 115 (2016) 337–342.

[14] S.H. Araghi, M.H. Entezari, Amino-functionalized silica magnetite nanoparticles for the simultaneous removal of pollutants from aqueous solution, Appl. Surf. Sci., *333* (2015) 68–77.

[15] T.S. Anirudhan, F. Shainy, Adsorption behaviour of 2-mercaptobenzamide modified itaconic acid-grafted-magnetite nanocellulose composite for cadmium(II) from aqueous solutions, J. Ind. Eng. Chem., 32 (2015) 157–166.

[16] M.H.P. Wondracek, A.O. Jorgetto, A.C.P. Silva, J.R. Ivassechen, J.F. Schneider, M.J. Saeki, V.A. Pedrosa, W.K. Yoshito, F. Colauto, W.A. Ortiz, G.R. Castro, Synthesis of mesoporous silica-coated magnetic nanoparticles modified with 4-amino-3-hydrazino-5-mercapto-1,2,4-triazole and its application as Cu(II) adsorbent from aqueous samples, Appl. Surf. Sci., *367* (2016) 533–541.

[17] I. Mohmood, C.B. Lopes, I. Lopes, D.S. Tavares, A.M.V.M Soares, A.C. Duarte, T. Trindade, I. Ahmad, E. Pereira, Remediation of mercury contaminated saltwater with functionalized silica coated magnetite nanoparticles, Sci. Total Environ., 557–558 (2016) 712–721.

[18] O. Duman, C. Özcan, T.G. Polat, S. Tunç, Carbon nanotube-based magnetic and non-magnetic adsorbents for the high-efficiency removal of diquat dibromide herbicide from water: OMWCNT, OMWCNT-Fe_3O_4 and OMWCNT-κ-carrageenan-Fe_3O_4 nanocomposites, Environ. Pollut., 244 (2019) 723–732.

[19] O. Duman, S. Tunç, T.G. Polat, B.K. Bozoğlan, Synthesis of magnetic oxidized multiwalled carbon nanotube-κ-carrageenan-Fe_3O_4 nanocomposite adsorbent and its application in cationic Methylene Blue dye adsorption, Carbohydr. Polym., 147 (2016) 79–88.

[20] Q. Zhang, T. Lu, D.M. Bai, D.Q. Lin, S.J. Yao, Self-immobilization of a magnetic biosorbent and magnetic induction heated dye adsorption processes, Chem. Eng. J., 284 (2016) 972–979.

[21] H. Wang, Y. Liu, J. Ifthikar, L. Shi, A. Khan, Z. Chen, Towards a better understanding on mercury adsorption by magnetic bio-adsorbents with γ-Fe_2O_3 from pinewood sawdust derived hydrochar: Influence of atmosphere in heat treatment, Bioresour. Technol., 256 (2018) 269–276.

[22] D. Sud, G. Mahajan, M.P. Kaur, Agricultural waste material as potential adsorbent for sequestering heavy metal ions from aqueous solutions - a review, Bioresour. Technol., 99 (2008) 6017–6027.

[23] D. Mohan, A. Sarswat, V.K. Singh, M. Alexandre-Franco, C.U. Pittman Jr, Development of magnetic activated carbon from almond shells for trinitrophenol removal from water, Chem. Eng. J., 172 (2011) 1111–1125.

[24] M.M. Montazer-Rahmati, P. Rabbani, A. Abdolali, A.R. Keshtkar, Kinetics and equilibrium studies on biosorption of cadmium, lead, and nickel ions from aqueous solutions by intact and chemically modified brown algae, J. Hazard. Mater., 185 (2011) 401–407.

[25] N. Chen, Z. Zhang, C. Feng, M. Li, D. Zhu, N. Sugiura, Studies on fluoride adsorption of iron-impregnated granular ceramics from aqueous solution, Mater. Chem. Phys., 125 (2011) 293–298.

[26] Z. Chen, M. Ma, M. Han, Biosorption of nickel and copper onto treated alga (*Undaria pinnatifida*): application of isotherm and kinetic models, J. Hazard. Mater., 155 (2008) 327–333.

[27] S.J. Mousavi, M. Parvini, M. Ghorbani, Adsorption of heavy metals (Cu^{2+} and Zn^{2+}) on novel bifunctional ordered mesoporous silica: optimization by response surface methodology, J. Taiwan Inst. Chem. Eng., 84 (2018) 123–141.

[28] J. Georgina, G.L. Dottob, M.A. Mazuttib, E.L. Folettob, Preparation of activated carbon from peanut shell by conventional pyrolysis and microwave irradiation-pyrolysis to remove organic dyes from aqueous solutions, J. Environ. Chem. Eng., 4 (2016) 266–275.

[29] S. Naeimi, H. Faghihian, Performance of novel adsorbent prepared by magnetic metal-organic framework (MOF) modified by potassium nickel hexacyanoferrate for removal of Cs^+ from aqueous solution, Sep. Purif. Technol., 175 (2017) 255–265.

[30] H.P.S. Abdul-Khalil, M. Jawaid, P. Firoozian, U. Rashid, A. Islam, H. Akil, Activated carbon from various agricultural wastes by chemical activation with KOH: preparation and characterization, J. Biobased Mater. Bioenergy, 7 (2013) 1–7.

[31] Buhani, Suharso, F. Luziana, M. Rilyanti, Sumadi, Production of adsorbent from activated carbon of palm oil shells coated by Fe_3O_4 particle to remove crystal violet in water, Desal. Water Treat., 171 (2019) 281–293.

[32] Y. Lin, H. Chen, K. Lin, B. Chen, C. Chiou, Application of magnetic modified with amino groups to adsorb copper ion in aqueous solution, J. Environ. Sci., 23 (2011) 44–50.

[33] V.K. Gupta, A. Rastogi, Biosorption of lead from aqueous solution by green algae *Spirogyra* species: kinetics and equilibrium studies, J. Hazard. Mater., 152 (2008) 407–414.

[34] A.H. AbdEl-Salam, H.A. Ewais, A.S. Basaleh, Silver nanoparticles immobilized on the activated carbon as efficient adsorbent for removal of crystal violet dye from aqueous solutions. A kinetic study, J. Mol. Liq., 248 (2017) 833–841.

[35] A.M. Aljeboree, A.F. Alkaim, A.H. Al-Dujaili, Adsorption isotherm, kinetic modeling and thermodynamics of crystal violet dye on coconut husk-based activated carbon, Desal. Water Treat., 53 (2015) 3656–3667.

[36] J. Gong, T. Liu, X. Wang, X. Hu, L. Zhang, Efficient removal of heavy metal ions from aqueous systems with the assembly of anisotropic layered double hydroxide nanocrystals@carbon nanosphere, Environ. Sci. Technol., 45 (2011) 6181–6187.

[37] T. Hou, L. Yan, J. Li, Y. Yang, L. Shan, X. Meng, X. Li, Y. Zhao, Adsorption performance and mechanistic study of heavy metals by facile synthesized magnetic layered double oxide/carbon composite from spent adsorbent, Chem. Eng., 384 (2020) 123331.

[38] E. Ayranci, O. Duman, Structural effects on the interactions of benzene and naphthalene sulfonates with activated carbon cloth during adsorption from aqueous solutions, Chem. Eng. J., 156 (2010) 70–76.

[39] O. Duman, S. Tunç, T.G. Polat, Determination of adsorptive properties of expanded vermiculite for the removal of CI Basic Red 9 from aqueous solution: kinetic, isotherm and thermodynamic studies, Appl. Clay Sci., 109 (2015) 22–32.

[40] K.P. Singh, S. Gupta, A.K. Singh, S. Sinha, Optimizing adsorption of crystal violet dye from water by magnetic nanocomposite using response surface modeling approach, J. Hazard. Mater., 186 (2011) 1462–1473.

[41] M. Achak, A. Hafidi, N. Ouazzani, S. Sayadi, L. Mandi, Low cost biosorbent "banana peel" for the removal of phenolic compounds from olive mill wastewater: kinetic and equilibrium studies, J. Hazard. Mater., 166 (2009) 117–125.

[42] Buhani, M. Puspitarini, Rahmawaty, Suharso, M. Rilyanti, Sumadi, Adsorption of phenol and methylene blue in solution by oil palm shell activated carbon prepared by chemical activation, Orient. J. Chem., 34 (2018) 2043–2050.

[43] Y.D. Liang, Y.J. He, T.T. Wang, L.H. Lei, Adsorptive removal of gentian violet from aqueous solution using $CoFe_2O_4$/activated carbon magnetic composite, J. Water Process. Eng., 27 (2019) 77–88.

[44] M. Dogan, H. Abak, M. Alkan, Adsorption of methylene blue onto hazelnut shell: kinetics, mechanism and activation parameters, J. Hazard. Mater., 164 (2009) 172–181.

[45] N.A. Oladoja, A.K. Akinlabi, Congo red biosorption on palm kernel seed coat, Ind. Eng. Chem. Res., 48 (2009) 6188–6196.

[46] X. Xin, Q. Wei, J. Yang, L. Yan, R. Feng, G. Chen, B. Du, H. Li, Highly efficient removal of heavy metal ions by amine-functionalized mesoporous Fe_3O_4 nanoparticles, Chem. Eng. J., 184 (2012) 132–140.

[47] I. Larraza, M. Lŏpez-Gŏnzales, T. Corrales, G. Marcelo, Hybrid materials: Magnetite-ployethyenimine-montromolillonite, as magnetic adsorbents for Cr (VI) water treatment, J. Colloid Interface Sci., 385 (2012) 24–33.

[48] Y. Shao, L. Zhou, C. Bao, J. Ma, M. Liu, F. Wang, Magnetic responsive metal–organic frameworks nanosphere with core–shell structure for highly efficient removal of methylene blue, Chem. Eng. J., 283 (2016) 1127–1136.

[49] Y.S. Ho, J.F. Porter, G. McKay, Equilibrium isotherm studies for the sorption of divalent metal ions onto peat: copper, nickel, and lead single component systems, Water Air Soil Pollut., 141 (2002) 1–33.

[50] O. Duman, E. Ayranci, Structural and ionization effects on the adsorption behaviors of some anilinic compounds from aqueous solution onto high-area carbon-cloth, J. Hazard. Mater., 120 (2005) 173–181.

[51] O. Duman, E. Ayranci, Adsorption characteristics of benzaldehyde, sulphanilic acid, and p-phenolsulfonate from water, acid, or base solutions onto activated carbon cloth, Sep. Sci. Technol., 41 (2006) 3673–3692.

[52] E. Ayranci, O. Duman, Adsorption behaviors of some phenolic compounds onto high specific area activated carbon cloth, J. Hazard. Mater., 124 (2005) 125–132.

[53] S. Hamidzadeh, M. Torabbeigi, S.J. Shahtaheri, Removal of crystal violet from water by magnetically modified activated carbon and nanomagnetic iron oxide, J. Environ. Health Sci. Eng., 13 (2015) 1–7.

[54] Buhani, Suharso, H. Satria, Hybridization of *Nannochloropsis* sp. biomass-silica through sol-gel process to adsorb Cd(II) ion in aqueous solutions, Eur. J. Sci. Res., 51 (2011) 467–476.

[55] U. Farooq, M.A. Khan, M. Athar, J.A. Kozinski, Effect of modification of environmentally friendly biosorbent wheat (*Triticum aestivum*) on the biosorptive removal of cadmium(II) ions from aqueous solution, Chem. Eng. J., 171 (2011) 400–410.

[56] T.M. Alslaibi, I. Abustan, M.A. Ahmad, A.A. Foul, Cadmium removal from aqueous solution using microwaved olive stone activated carbon, J. Environ. Chem. Eng., 1 (2013) 589–599.

[57] R. Sitko, P. Janik, B. Zawisza, E. Talik, E. Margui, I. Queralt, Green approach for ultratrace determination of divalent metal ions and arsenic species using total-reflection X-ray fluorescence spectrometry and mercapto-modified graphene oxide nanosheets as a novel adsorbent, Anal. Chem., 87 (2015) 3535–3542.

[58] Z.L. Du, T. Zheng, P. Wang, L.L. Hao, Y.X. Wang, Fast microwave-assisted preparation of a low-cost and recyclable carboxyl modified lignocellulose-biomass jute fiber for enhanced heavy metal removal from water, Bioresour. Technol., 201 (2016) 41–49.

[59] H.Y. Choi, J.H. Bae, Y. Hasegawa, S. An, I.S. Kim, H. Lee, M. Kim, Thiol-functionalized cellulose nanofiber membranes for the effective adsorption of heavy metal ions in water, Carbohydr. Polym., 234 (2020) 115881.

[60] B.L. Zhang, W. Qiu, P.P. Wang, Y.L. Liu, J. Zou, L. Wang, J. Ma, Mechanism study about the adsorption of Pb(II) and Cd(II) with iron-trimesic metal–organic frameworks, Chem. Eng. J., 385 (2020) 123507.

[61] H. Liu, X. Wang, G. Zhai, J. Zhang, C. Zhang, B. Nan, C. Cheng, Preparation of activated carbon from lotus stalks with the mixture of phosphoric acid and pentaerythritol impregnation and its application for Ni(II) sorption, Chem. Eng. J., 209 (2012) 155–162.